Bioorganic & Medicinal Chemistry 19 (2011) 2650–2658

Contents lists available at ScienceDirect

Bioorganic & Medicinal Chemistry

journal homepage: www.elsevier.com/locate/bmc

Extending SAR of bile acids as FXR ligands: Discovery of 23-*N*-(carbocinnamyloxy)-3α,7α-dihydroxy-6α-ethyl-24-nor-5β-cholan-23-amine

Antimo Gioiello [a], Antonio Macchiarulo [a], Andrea Carotti [a], Paolo Filipponi [a], Gabriele Costantino [b], Giovanni Rizzo [c], Luciano Adorini [c], Roberto Pellicciari [a,*]

[a] Dipartimento di Chimica e Tecnologia del Farmaco, Università degli Studi di Perugia, Via del Liceo 1, 06123 Perugia, Italy
[b] Dipartimento Farmaceutico, Università degli Studi di Parma, V.le G.P. Usberti 27/A, I-43124 Parma, Italy
[c] Intercept Pharmaceuticals Italia Srl, Via Togliatti, 06073 Corciano, Perugia, Italy

ARTICLE INFO

Article history:
Received 3 January 2011
Revised 28 February 2011
Accepted 3 March 2011
Available online 10 March 2011

Keywords:
FXR
Bile acid
Carbamate
RMDS
Allosteric site

ABSTRACT

Within our efforts in the discovery of novel potent and selective ligands for the FXR receptor, 23-*N*-(carbocinnamyloxy)-3α,7α-dihydroxy-6α-ethyl-24-nor-5β-cholan-23-amine was synthesized and evaluated for its ability to activate and modulate the biological response of the receptor. Alphascreen and RT-PCR revealed that the 6α-ethyl-24-norcholanyl-23-amine derivate behaves as full FXR agonist endowed with high binding affinity and efficacy, representing a promising lead candidate for further optimization. In addition, docking studies provide new insights into the molecular basis governing the partial and full agonist activity at FXR.

1. Introduction

The farnesoid-X receptor (FXR, also known as BAR; *NR1H4*) belongs to the superfamily of intracellular ligand-activated transcription factors that are involved in many physiological, developmental and toxicological processes.[1] Although initially characterized as a metabolic nuclear receptor activated by farnesol,[2] since 1999 FXR is considered a key nuclear receptor for bile acids (BAs), with chenodeoxycholic acid (CDCA, **1**, Fig. 1) being its most potent endogenous agonist.[3] FXR is abundantly expressed in tissues exposed to BAs, such as liver, intestine, kidneys, and in the ileal epithelium along the intestinal tract, where BAs are mainly absorbed.[2,4]

Two FXR genes exist in lower mammalians including rodents, rabbits and dogs, that encode for α and β types of receptor. While FXRβ is a pseudogene in humans and primates,[5] the expression of FXRα gene further originates four isoforms (FXRα1-4) as a result of alternative splicing and different promoters.[6] Although the physiological importance of each isoform is still unclear, it is known that the four isoforms of FXRα exhibit diverse DNA binding and coregulator recruitment.[7] Over the past decade, a number of evidences have shown the key role of FXR in regulating different metabolic pathways, including the homeostasis of BAs, lipids and glucose,[1] as well as in liver regeneration.[8]

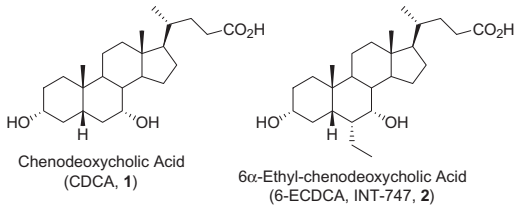

Figure 1. CDCA derivatives as FXR agonists.

The regulation of BA metabolism, for instance, occurs at three complementary levels of action: (i) decreasing the BA synthetic pathway; (ii) supporting the bile flow in the enterohepatic circulation; (iii) increasing the clearance of toxic biliary constituents. At the first level, FXR negatively regulates the BA synthetic pathway through the down-regulation of the rate-limiting enzyme CYP7A1, and the repression of CYP8B1, another key enzyme in BA synthesis.[9] Interestingly, the repression of CYP7A1 occurs through the activation of FXR in the liver and intestine (Gut-Liver Axis) via the induction of the small heterodimer partner (SHP) and the activation of the fibroblast growth factor (mouse FGF15/human

* Corresponding author. Tel.: +39 075 585 5120; fax: +39 075 585 5124.
E-mail address: rp@unipg.it (R. Pellicciari).

0968-0896/$ - see front matter © 2011 Elsevier Ltd. All rights reserved.
doi:10.1016/j.bmc.2011.03.004

FGF19) signaling pathway.[10] In addition, FXR inhibits HMG-CoA reductase and down-regulates lanosterol 14α-demethylase which are both important in the synthesis of cholesterol, the endogenous precursor of BAs.[11] At the second level of action, FXR supports bile flow in the enterohepatic circulation through the induction of genes involved in BA secretion from liver, such as the bile salt export pump (BSEP) and the multidrug resistant-associated protein 2 (MRP2); the down-regulation of genes involved in the import of BAs into the liver, that include the organic anion transporting polypeptide-2 and -8 (OATP-2 and -8) and the sodium-dependent taurocholate co-transporting protein (NTCP); the regulation of genes involved in the transport of BAs in the intestine such as the intestinal bile acid binding protein (IBABP), the apical sodium-dependent bile acid cotransporter (ASBT) and the organic solute transporters-α and -β (OST-α and -β).[12] Finally, FXR increases the clearance of toxic biliary constituents trough the regulation of additional genes, including the dehydroepiandrosterone sulfotransferase (SULT2A1), the bile acid N-acetyltransferase (BAT), and the bile acid CoA synthetase (BACS).[1d]

The unraveling of the physiological functions of FXR has disclosed unprecedented opportunities for this receptor as drug target in different therapeutic areas such as liver diseases, metabolic syndrome and, more recently, hepatocarcinogenesis.[1] In this scenario, a number of molecules have been discovered, including both non-steroidal and steroidal compounds that were able to bind and interact with the ligand binding domain (LBD) of FXR in different ways, leading to ligand and promoter selectivity for the FXR-mediated gene transcription.[1e,f] While non-steroidal compounds have been identified using high-throughput screenings of chemical libraries eventually filtered for lead-like and/or drug-like properties,[1a,b,f,13] the identification of FXR steroidal modulators has mostly relied on a design strategy based on extensive modifications of the BA body and side chain.[14] Embracing the latter approach, we have developed thorough structure activity relationships of BA derivatives as FXR ligands. These studies unveiled a striking increase of agonist activity at the receptor when introducing an ethyl group in the C_6 alpha position of CDCA (**1**), thereby disclosing 6-ECDCA (INT-747, **2**) as the most potent and orally bioavailable agonist for FXR.[14e] 6-ECDCA (**2**) is being advanced in clinical studies for non-alcoholic steatohepatitis (NASH), and recent results of phase II clinical studies for primary biliary cirrhosis (PBC) show a significant reduction of primary endpoint biomarkers of the clinical status and progression of the disease.

While significant progress has been made towards the discovery of potent agonists, great efforts are still needed for the development of selective FXR modulators (referred to as 'selective bile acid receptor modulators', SBARMs), compounds able to regulate individual or a cluster of FXR target genes.[1f,g] These peculiar FXR modulators will offer the possibility to reduce the pleiotropism of the receptor's action and to explore novel therapeutic opportunities which cannot be reacted by the use of FXR activators. In pursing this aim, we have reported that the substitution of the carboxylic tail of CDCA (**1**) with diverse substituted carbamate moieties was able to affect the agonist potency of BAs at FXR, leading to a broad range of efficacy in both cell-free FRET and cell-based luciferase assays (Fig. 2).[14b,c] Docking experiments suggested for the first time that the LBD of FXR contains two contiguous pockets: the steroid binding pocket and the 'back door' pocket.[14b] The former, in particular, accommodates the BA body and C_{24} side chain, whereas the latter lodges the extended side chain substitution. Although the significance of this observation and its possible extension to other members of the nuclear receptor superfamily deserves further investigation, we demonstrated that it is possible to achieve full agonism, partial agonism, or antagonism by modifying a part of the molecule that is not directly interacting with any of the LBD elements known to affect coactivator binding.

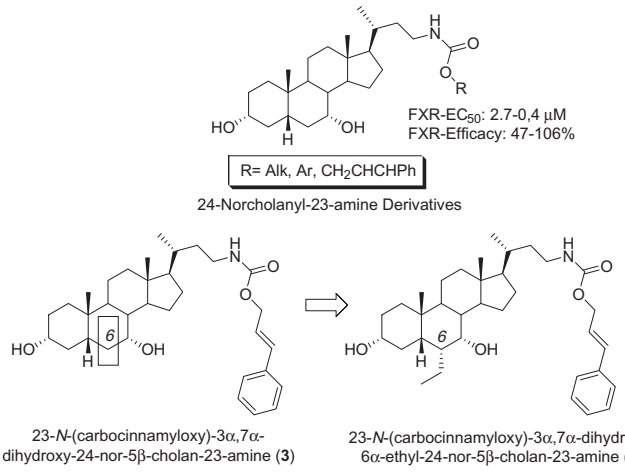

Figure 2. Structure and FXR activity of 24-norcholanyl-23-amine derivatives.

With the aim of shedding light on the existence of any cross-talk between the steroid binding pocket and the 'back door' pocket responsible for the transactivation properties of FXR, and continuing our efforts in the identification of FXR selective modulators, in this study we report the synthesis, biological evaluations and molecular modeling studies of 23-*N*-(carbocinnamyloxy)-3α,-7α-dihydroxy-6α-ethyl-24-nor-5β-cholan-23-amine (**4**) (Fig. 2). We were, indeed, attracted by the interesting biological properties of 23-*N*-(carbocinnamyloxy)-3α,7α-dihydroxy-24-nor-5β-cholan-23-amine (**3**), a carbamate BA derivative 10-fold more potent than CDCA (**1**) but endowed with partial agonism in FRET-assay (EC_{50} = 0.62 μM, efficacy = 63%).[14b] We focused our attention, in particular, on the incorporation of the crucial 6α-ethyl group in the scaffold of **3** as key structural element to improve the potency of the resulting compound.

2. Results

2.1. Chemistry

The synthesis of **4** is outlined in Scheme 1.[14b,16d] Treatment of methyl 7-keto-deoxycholate **5** with LDA in THF at −78 °C followed by reaction of the enolate thus formed with trimethylchlorosilane (TMSCl) afforded the corresponding silyl enolether **6**, in nearly quantitative yield. Aldol-type addition of intermediate **6** with acetaldehyde in the presence of $BF_3{\cdot}OEt_2$ at −60 °C in CH_2Cl_2 gave the desired methyl 3α-hydroxy-6-ethylidene-7-keto-5β-cholan-24-oate (**7**) (*Z*:*E*, 85:15) in 80% yield. Hydrogenolysis of **7** with platinum dioxide (PtO_2) in a mixture of glacial acetic acid/hydrochloric acid, followed by alkali hydrolysis (10% NaOH in refluxing methanol) afforded selectively 3α-hydroxy-6α-ethyl-7-keto-5β-cholan-24-oic acid in good yield. Selective reduction of the C_7-ketone with sodium borohydride ($NaBH_4$) in a mixture of THF/H_2O at room temperature afforded the 6-ECDCA (**2**), in 58% overall yield (from **5**) (Scheme 1). Protection of the 3,7-hydroxy groups of 6-ECDCA (**2**) was achieved by reaction with formic acid in the presence of catalytic amount of *p*-toluensulfonic acid (*p*-TSA) in refluxing benzene (96% yield). 3α,7α-Diformyl CDCA (**8**) was converted into the corresponding acyl azides, via acyl chloride intermediate (oxalyl chloride), followed by treatment with aqueous sodium azide at 0 °C. The crude acyl azide mixture was then refluxed in dry toluene to give the corresponding isocyanate **9** by Curtius rearrangement. Addition of *t*-cinnamyl alcohol (1.2 equiv) and removal of the formyl groups by hydrolysis with potassium carbonate in methanol at room temperature gave the desired 23-*N*-(carbocinnamyloxy)-

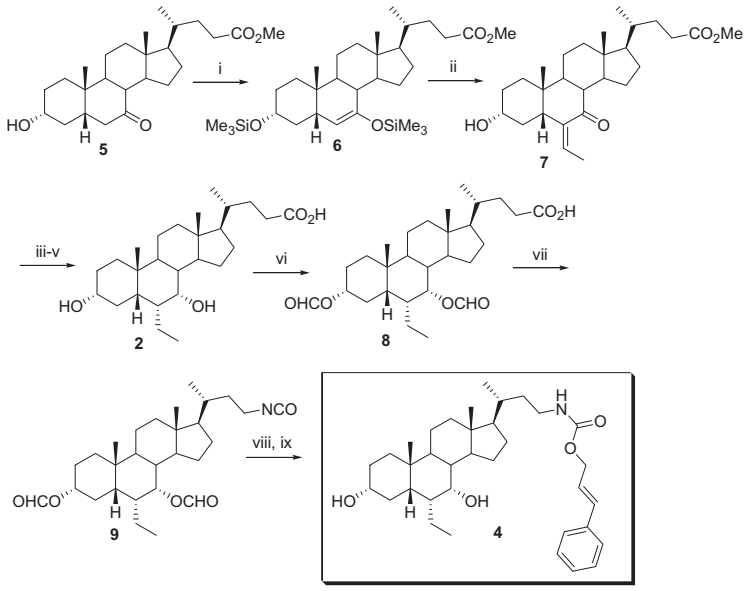

Scheme 1. Synthesis of 23-*N*-(carbocinnamyloxy)-3α,7α-dihydroxy-6α-ethyl-24-nor-5β-cholan-23-amine (**4**). Reagent and conditions: (i) LDA, TMSCl, Et_3N, THF, −78 °C; (ii) MeCHO, $BF_3{\cdot}OEt_2$, CH_2Cl_2, −60 °C; (iii) H_2, PtO_2, AcOH/HCl, rt; (iv) NaOH, MeOH, refl.; (v) $NaBH_4$, THF/H_2O, rt; (vi) HCO_2H, *p*-TSA, benzene, refl.; (vii) (a) $(COCl)_2$, 45 °C; (b) NaN_3, H_2O, acetone, 0 °C; (c) toluene, refl.; (viii) *t*-cinnamoyl alcohol, toluene, reflux; (ix) K_2CO_3, MeOH, rt.

3α,7α-dihydroxy-6α-ethyl-24-nor-5β-cholan-23-amine (**4**), in 48% overall yield (Scheme 1).

2.2. Biology

In order to characterize the binding potency of **3** and **4** as ligands for FXR, we used a coactivator recruitment assay (Alphascreen),[15] in which the ligand induces the recruitment of a coactivator to the LBD of human FXR. In this assay, **4** shows a very potent agonist activity on FXR, with an EC_{50} = 0.15 μM and efficacy = 290%, while **3** confirms to be a partial agonist with an EC_{50} = 0.9 μM and efficacy = 55% (Table 1). The effect on FXR activation of **3** and **4** was then tested in cell-based transactivation assay using a human hepatic cell line (HepG2) transfected with the full-length FXR and FXRE$(IR1)_3$-Luc. As a result, compound **4** shows full agonistic activity on FXR at 1 μM, comparable to that of 6-ECDCA (**2**), whereas **3** proves to be only a partial agonist at FXR even at a concentration of 20 μM (Fig. 3).

In addition, since natural BA and BA derivatives are known to activate the TGR5 receptor,[16] we investigated if the 24-norcholanyl-23-amine derivatives **3** and **4** could bind also the metabotropic receptor. By using time-resolved fluorescence resonance energy transfer (TR-FRET) we have determined the increase of intracellular levels of cAMP in human enteroendocrine cell line (NCI-H716) physiologically expressing TGR5. As shown in Table 1, both derivatives **3** and **4** increase cAMP at high dose indicating only a weak or absent TGR5 agonist activity.

Table 1
FXR and TGR5 activities of bile acid derivatives[a]

Compound	FXR		TGR5
	EC_{50} ± SD	Efficacy[b]	EC_{50} ± SD
CDCA (**1**)	21.0 ± 3.5	100	30 ± 5
6-ECDCA (**2**)	0.20 ± 0.05	245	20 ± 4
3	0.90 ± 0.04	55	>100
4	0.15 ± 0.05	290	55.0 ± 5.7

Data represents average values of at least three independent experiments.
[a] Units are μM for EC_{50} and% for efficacy.
[b] Units are % of 20 μM **1**.

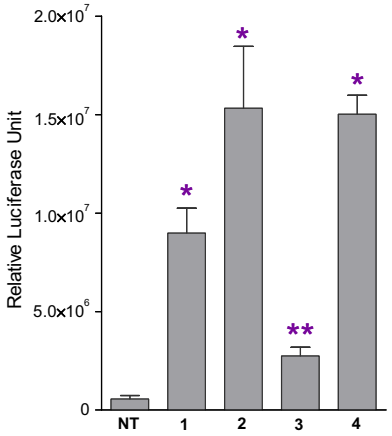

Figure 3. Biological activity of norcholanylamine derivatives **3** and **4** in FXR transactivation assay. Cells were exposed to 20 μM of **1** and **3** and 1 μM of **2** and **4**. Luciferase activity was normalized using renilla luciferase as the internal control. Relative luciferase expression in untreated cells (NT) is shown.

Next, we investigated their gene expression profile, using a quantitative real-time PCR and assessing the mRNA expression of selected FXR target genes. In particular, we analyzed the expression of SHP, BSEP, Ostβ, and Cyp7α1 in HepG2 cells (Fig. 4).

The results indicate that both derivatives **3** and **4** induce the expression of SHP, BSEP, and Ostβ genes, while down-regulating the expression of Cyp7A1 (Fig. 4). However, while the effect of **3** in modulating FXR gene expression was less efficient than CDCA (**1**) and 6-ECDCA (**2**), **4** resulted to be more potent than **2** in activating the receptor and regulating FXR target genes.

2.3. Molecular modeling

Docking experiments were performed on **3** and **4** in the attempt to identify the molecular basis responsible of their partial and full agonism at FXR. In the case of PPARγ modulators, it has been reported that full agonists stabilize the H12 helix whereas partial agonists mainly act on the H3 stabilization.[17] Accordingly, we

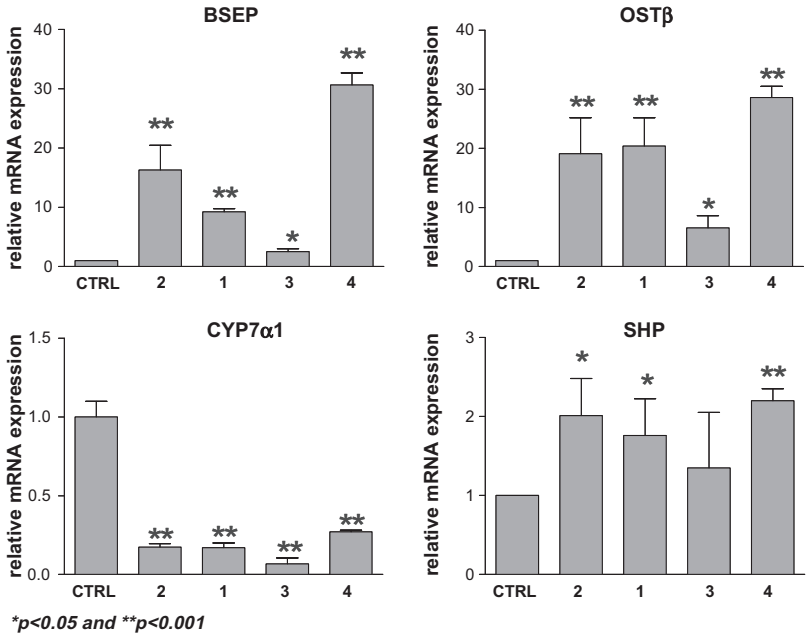

Figure 4. Quantitative gene expression induced by **3** and **4** measured by using real-time PCR. HepG2 cells were treated with vehicle alone, **3** at 20 μM concentration, and **4** at 1 μM concentration. CDCA (**1**) and 6-ECDCA (**2**) were used as reference standard at 20 and 1 μM, respectively.

Table 2
Results of docking experiments of compounds **3** and **4** into the LBD of FXR.

Compound	Glide XP score S2	Backbone RMSD S2 (Å)	Glide XP Score S3	Backbone RMSD S3 (Å)
3	−11.75	1.97 ± 0.13	−11.58	2.44 ± 0.16
4	−13.57	1.88 ± 0.11	−13.17	2.06 ± 0.16

deemed of interest to investigate the existence of a similar scenario in the case of FXR to explain the pharmacological profiles of **3** and **4**. To this end, we firstly docked each compound into the LBD of FXR (Table 2).

As a result, the two ligands bind to the steroidal binding site (S1) with the steroid nucleus, while their extended side chain fills two alternative pockets: the 'back door' site (S2), or a solvent exposed site (S3). While the 'back door' site is composed of Tyr257, Phe298 and Thr383, S3 is mostly exposed to the solvent, with only three residues (Asn268, Lys335 and Pro338) being the possible anchoring points (Fig. 5). The inspection of the binding energy scores (Glide XP scores, Table 2) suggests that the occupancy of the 'back door' site (S2) is slightly preferred over the S3 site for both compounds, with **4** showing higher scores than **3** in agreement to its potency. However, given the almost identical scores of compounds **3** and **4** in S2 and S3, we deemed advisable to consider as plausible all the four solutions at this stage. Accordingly, four molecular dynamic experiments were carried out in water solvated boxes with periodic boundary conditions for 10 ns. The analysis of the mean interaction energies between the ligand and the protein in each simulation suggests that the occupancy of the 'back door' site (S2) by the extended side chain is more favorable than that of the S3 site, with the energetic differences being of −8.55 and −17.82 kcal/mol in the case of compound **3** and **4**, respectively. The preference of this binding solution is further supported by the lower root mean square deviation (RMSD) of the backbone atoms as calculated in the trajectories from the starting docked pose: RMSD = 1.97 ± 0.13 Å for **3** binding S2 versus RMSD = 2.44 ± 0.16 Å for **3** binding S3; RMSD = 1.88 ± 0.11 Å for **4** binding S2 versus RMSD = 2.06 ± 0.16 Å for **4** binding S3.

Thus, based on the above results, we selected as plausible the binding pose of compounds **3** and **4** with the BA scaffold occupying the steroidal binding site (S1), and the extended side chain fitting the 'back door' site (S2). This binding solution was instrumental to investigate the stability of helices H3 and H12 as molecular determinants for full and partial agonism of compounds **3** and **4** at FXR (Fig. 6). In particular, this was achieved by calculating the mean RMSD values of the backbone atoms constituting the residues of helices H3 (residues Ser276-Lys300) and H12 (residues Thr459–Trp466) from the starting agonistic conformation of the receptor. Thus, it was found that **3** and **4** stabilize helix H12 to different values of RMSD (**3** RMSD = 1.59 ± 0.41 Å; **4** RMSD = 1.46 ± 0.43 Å), albeit the large standard deviations suggest the presence of high fluctuating residues. In addition, compounds **3** and **4** show a diverse stabilization pattern for helix H3, with the partial agonist inducing a larger stabilization than the full agonist (**3** RMSD = 1.60 ± 0.22 Å; **4** RMSD = 1.84 ± 0.19 Å), and in both cases the presence of less fluctuating residues with the respect to helix H12.

3. Discussion

While substitution of the carboxylic group of CDCA (**1**) by an amino group preserved both the potency and efficacy of the parent derivative **1**, carbamoylation of the distal C_{24}-amino derivative with a cinnamyl functionality gave the corresponding carbamate derivative **3**, which displayed the profile of a partial FXR agonist (Table 1).[14b,14c] Further insertion of an ethyl group in position C6α resulted in 23-*N*-(carbocinnamyloxy)-3α,7α-dihydroxy-6α-ethyl-24-nor-5β-cholan-23-amine (**4**), which was endowed with a high FXR binding affinity and, surprisingly, with a better efficacy when compared to **2**. Consistent with this finding, RT-PCR experiments revealed that **4** is a potent FXR agonist, thereby regulating

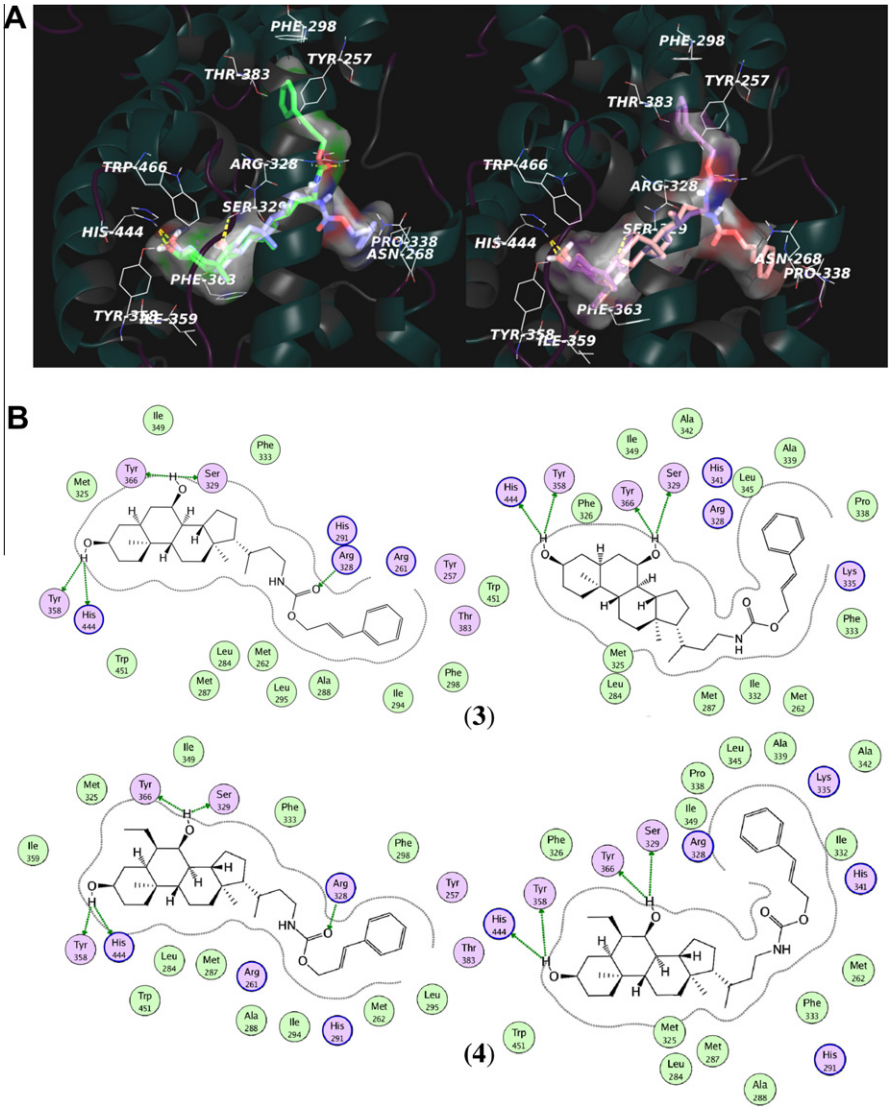

Figure 5. (A) Docking poses of compounds **3** (left) and **4** (right). The two ligands display two alternative binding modes: one with the carbamic moiety oriented towards S2 (**3**, green; **4**, violet) and another pointing to S3 (**3**, bluet, **4**, pink). Hydrogen bonds are displayed in yellow and the key residues are labeled. (B) 2D representations of the compounds **3** and **4** in the two proposed binding modes (left: S2 oriented; right: S3 oriented). Hydrogen bonds are displayed with green arrows, polar and charged residues are shown in pink and lipophilic residues are shown in green.

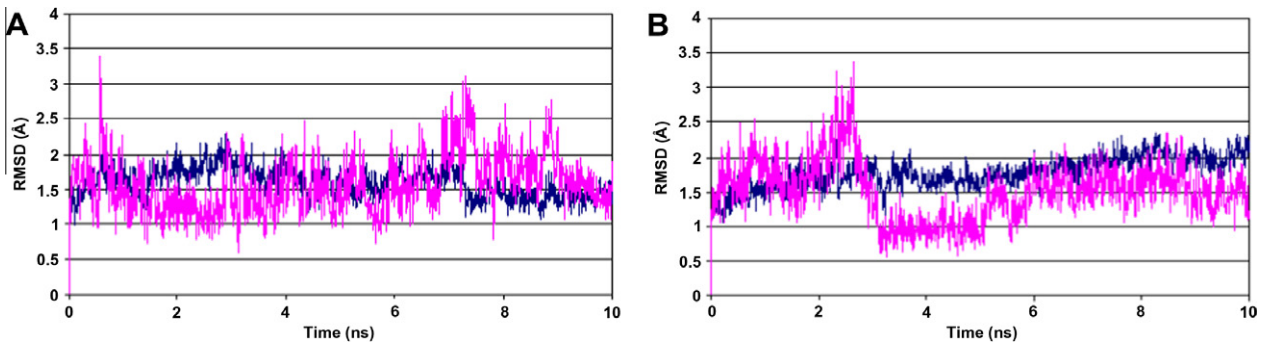

Figure 6. Stability of helices H3 (blue) and H12 (magenta) as expressed by the RMSD (Å) of the relative backbone atoms during the molecular dynamic simulations of compounds **3** (left) and **4** (right).

FXR target gene expression. At the cellular level, while both norcholanylamine derivatives **3** and **4** gave a similar gene expression profile with respect to the endogenous FXR agonist CDCA (**1**), **4** was found to be more effective than 6-ECDCA (**2**), considered so far the most potent BA-based agonist for FXR. In particular, a strong induction of BSEP and OSTβ expression was observed indicating that **4** presumably leads to an increase of BA secretion and efflux in ileum and other ASBT-expressing tissues, while the

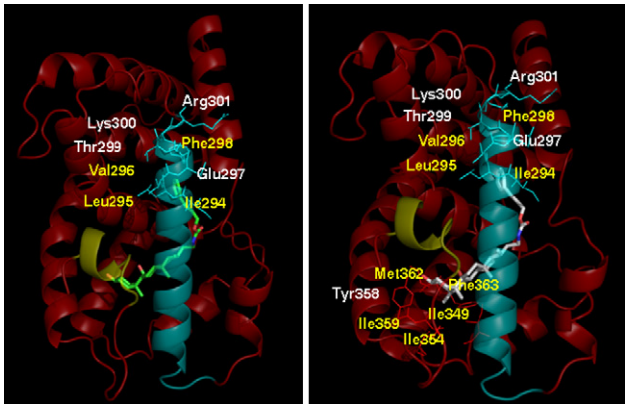

Figure 7. Proposed molecular basis for the different stabilization of helices H3 (yellow ribbon) and H12 (cyan ribbon) by compounds **3** (left) and **4** (right). Hydrophobic residues are labeled in yellow.

repression of CYP7A1 and the slight induction of SHP may result in a decreased BA synthesis. On the basis of these considerations, it could be speculated that such compounding effects is potentially positive to contrast hepatotoxicity induced by an excessive hepatic accumulation of BAs.

Docking experiments and molecular dynamic simulations provided the molecular basis for rationalizing the activity of the new derivatives. In particular, both compounds adopt similar binding poses into the LBD of FXR (Fig. 5), with the BA scaffold and the extended side chain occupying the steroid binding site (S1) and the "back door" site (S2) of the receptor, respectively. Furthermore, in agreement with previous studies reporting a helix H3 dependent mechanism for partial agonists at PPARγ, we found that the compound **3** promotes a stabilization of helices H3 and H12 whereas the full agonist **4** mostly stabilizes helix H12 (Fig. 7). While the stabilization of H12 by **4** occurs through an indirect mechanism mediated by the extension of the hydrophobic contacts between the ligand and the steroid binding site (S1) that ensue the insertion of the ethyl group (Fig. 7, right panel), more challenging is the explanation of the molecular basis underpinning the stabilization of H3 by compound **3** (Fig. 7, left panel). Helix H3 is indeed part of S2 through the residues Ile294, Leu295, Val296, Glu297, Phe298, Thr299, Lys300 and Arg301. The hypothesis is that, unlike compound **4** (H3 RMSD = 1.84 ± 0.19 Å), the occupancy of S2 by the partial agonist **3** may favor the packing of helix H3 to the binding site (H3 RMSD = 1.60 ± 0.22 Å) through its hydrophobic residues Ile294, Leu295, Val296 and Phe298. This is not observed with the full agonist **4** because the insertion of the ethyl group would conversely disrupt the packing of H3 to the steroid binding site (S1) (H3 RMSD = 1.84 ± 0.19 Å), while promoting the packing of H12 (H12 RMSD = 1.46 ± 0.43 Å) and the full activation of the receptor.

In conclusion, our study provides evidence that also in the case of FXR, partial agonists mainly act trough the stabilization of helix H3, a finding potentially fruitful to design new FXR modulators with different biological features and gene expression profiles. Moreover, 23-*N*-(carbocinnamyloxy)-3α,7α-dihydroxy-6α-ethyl-24-nor-5β-cholan-23-amine (**4**) revealed here represent a novel avenue in search of new BA derivatives as FXR ligands, and potentially could serve as a promising new lead for further optimization.

4. Experimental

4.1. Chemistry

4.1.1. General methods

Chemical reagents and solvents were obtained from commercial sources. When necessary, solvents were dried and purified by standard methods. Melting points were determined with an electrothermal apparatus and are uncorrected. NMR spectra were recorded on a Bruker AC 200 or 400 MHz spectrometer and the chemical shifts are reported in parts per million (ppm). The abbreviations used are as follows: s, singlet; br s, broad singlet; d, doublet; dd, double doublet; m, multiplet. IR spectra were recorded with a Pelkin-Elmer 1320 Spectrometer. Flash column chromatography was performed using Merck Silica Gel 60 (0.040–0.063 mm). Thin-layer chromatography was performed using glass plates coated with Silica Gel 60 F-254. Spots were visualized by staining and worming with phosphomolybdate reagent (5% solution in EtOH). All reactions were carried out under a nitrogen atmosphere. Purity of final compounds was determined by NMR and HPLC analysis. All tested compound showed an HPLC purity more than 98% in two different systems: (a) analytical column: Ultra aqueous RP-18 Restek (Polar Base Deactivated); eluent: H_2O/CH_3CN: 20:80 (v/v); flow rate: 1.5 mL/min; detection at 250 nm; (b) column Grace Smart RP-18; eluent: $H_2O/CH_3CN/CH_3OH$: 35:35:10 (v/v/v); flow rate: 1 mL/min; detection at 254 nM. The HPLC analyses were carried out with a EZ Start chromatography data software, a LC-10 ATVP pump, a SCL-10AVP system controller, a FCV-10ALVP low pressure gradient formation unit, a DGU-14A on-line degasser and a 7725i injector with a 20 mL stainless steel loop; DAD or SPD-10A variable-wavelength UV–vis were used as detectors. 23-*N*-(carbocinnamyloxy)-3α,7α-dihydroxy-24-nor-5β-cholan-23-amine (**3**) was prepared as previously reported.[14b]

4.1.2. Methyl 3α,7-dimethylsilyloxy-5β-cholan-6-en-24-oate (6)

To a solution of diisopropylamine (10.4 mL, 0.079 mol) in dry THF (50 mL) was added dropwise a solution of *n*-butyllithium (31.6 mL, 2.5 M in hexane) at −78 °C under nitrogen atmosphere. After 30 min, trimethylchlorosilane (18.0 mL, 0.097 mol) was added, and the resulting mixture was reacted for additional 10 min. A solution of methyl 3α-hydroxy-7-keto-5β-cholan-24-oate (5.0 g, 0.012 mol) in dry THF (18 mL) was added dropwise in 40 min. The system was kept to −78 °C for an additional 30 min, and then triethylamine (24.1 mL, 0.18 mol) was added. After 1 h the reaction mixture was allowed to warm to −20 °C, treated with aqueous saturated solution of $NaHCO_3$ (25 mL), and brought up to room temperature in 3 h. The organic phase was separated, and aqueous phase was extracted with EtOAc (3 × 25 mL). The combined organic phases were washed several times with saturated solution of $NaHCO_3$, water, and brine. After drying over anhydrous Na_2SO_4, the residue was evaporated under vacuum affording to a 6.6 g of crude compound: R_f = 0.86 (PET/EtOAc, 9:1); ^{1}H NMR (400 MHz, $CDCl_3$) δ 0.13-0.18 (m, 18H, 3-OSiMe$_3$ and 7-OSiMe$_3$), 0.70 (s, 3H, 18-CH_3), 0.84 (s, 3H, 19-CH_3), 0.94 (d, J = 6.36 Hz, 3H, 21-CH_3), 3.53 (m, 1H, 3-CH), 3.69 (s, 3H, CO_2CH_3), 4.75 ppm (dd, J_1 = 1.86 Hz, J_2 = 5.91 Hz, 1H, 6-CH). HRMS (+ESI) calcd for $C_{31}H_{57}O_4Si_2$ $(M+H)^+$: 549.3795; found: 549.3791.

4.1.3. Methyl-3α-hydroxy-6-ethylidene-7-keto-5β-cholan-24-oate (7)

To a cooled (−60 °C) and stirred solution of acetaldehyde (1.3 mL, 22.2 mmol) and methyl 3α,7-diitrimethylsyliloxy-5β-chol-6-en-24-oate (**6**) (6.6 g) in dry CH_2Cl_2 (20 mL) was added dropwise a solution of $BF_3{\cdot}OEt_2$ (0.044 mol) in 15 mL of CH_2Cl_2. The reaction mixture was stirred for 2 h at −60 °C and allowed to warm to room temperature. The mixture was quenched with a saturated aqueous solution of $NaHCO_3$ and extracted with CH_2Cl_2. The combined organic extracts were washed with brine, dried (Na_2SO_4) and concentrated under *vacuum*. The crude residue was dissolved in CH_2Cl_2 (45 mL), treated with HCl (3 N, 20 mL), and stirred at 0 °C for 1 h. The reaction mixture was quenched with a saturated aqueous solution of $NaHCO_3$ (50 mL) and extracted with CH_2Cl_2. The combined organic phases were

dried over Na_2SO_4 anhydrous, filtered and evaporated under reduced pressure. The crude residue was purified by flash chromatography on silica gel using PET/EtOAc 7:3 as eluent to afford 4.13 g of **7** (9.6 mmol, 80%). R_f 0.28 (CH_2Cl_2/MeOH, 97:3); ^{1}H NMR (400 MHz, $CDCl_3$) δ 0.63 (s, 3H, 18-CH_3), 0.92 (d, J = 6.26 Hz, 3H, 21-CH_3), 1.00 (s, 3H, 19-CH_3), 1.68 (d, J = 7.17 Hz, 3H, 2′-CH_3), 2.55-2.58 (dd, 1H, 5-CH), 3.56-3.69 (m, 4H, 3-CH and CO_2CH_3), 6.17 ppm (q, 1H, 1′-CH); ^{13}C NMR (100.6 MHz, $CDCl_3$+CD_3OD) δ 11.9, 12.6, 18.3, 21.2, 22.7, 25.84, 28.30, 29.60, 30.88, 30.92(×2), 34.34, 34.46, 35.10, 37.43, 38.82, 38.96, 43.45, 45.37, 48.57, 50.54, 51.40, 54.34, 70.38, 129.76, 143.20, 174.61, 204.79 ppm. HRMS (+ESI) calcd for $C_{27}H_{43}O_4$ $(M+H)^+$: 431.3163; found: 431.3165.

4.1.4. 3α,7α-Dihydroxy-6α-ethyl-5β-cholan-24-oic acid (6-ECDCA, 2)

A solution of methyl 3α-hydroxy-6-ethylidene-7-cheto-5β-cholan-24-oate (**7**) (4.0 g, 9.3 mmol) in glacial acetic acid/HCl (200/10 mL, v/v) was hydrogenised in presence of platinum oxide (0.4 g) at 32 psi for 24 h. The catalyst was filtered off and the filtrate was concentrated. The residue was taken into a mixture of water (200 mL) and EtOAc (150 mL) and neutralized with an aqueous saturated solution of $NaHCO_3$. The separated aqueous layer was extracted with EtOAc (3 × 150 mL). The combined organic phases were washed with brine, dried (Na_2SO_4) and evaporated under reduced pressure. The crude product was hydrolysed overnight using a methanol solution of sodium hydroxide (10%, 500 mL). The mixture was then concentrated under vacuum, diluted with water, acidified with HCl 11 N and extracted with ethyl acetate (3 × 150 mL). The collected organic phases were washed with brine, dried over Na_2SO_4 anhydrous and evaporated under reduced pressure. The residual was dissolved in a solution of THF/H_2O (500 mL, 4:1, v/v) and treated with $NaBH_4$ overnight at room temperature. After evaporation of the solvents the residue was diluted with water, acidified with HCl 3 N and extracted with CH_3Cl/MeOH 9:1 (3 × 150 mL). The combined organic phases were washed with brine, dried over Na_2SO_4 anhydrous and evaporated under reduced pressure. The crude residue was purified by flash chromatography on silica gel using dichloromethane/methanol (7:3, v/v) as eluent, to afford 2.8 g (6.7 mmol, 72%) of **2**. R_f 0.38 (acetone/CH_2Cl_2/AcOH, 30:60:10); mp: 108-110 °C; ^{1}H NMR (400 MHz, $CDCl_3$+CD_3OD) δ 0.67 (s, 3H, 18-CH_3), 0.90-0.93 (m, 6H, 2′-CH_3, 19-CH_3), 0.95 (d, J = 6.43 Hz, 3H, 21-CH_3), 3.42 (m, 1H, 3-CH), 3.72 ppm (s, 1H, 7-CH); ^{13}C NMR (100.6 MHz, $CDCl_3$+CD_3OD) δ 11.62, 11.76, 18.23, 20.73, 22.20, 23.12, 23.65, 28.15, 30.46(×2), 30.85, 33.19, 33.79, 35.39(×2), 39.57, 39.99, 41.15, 42.73, 45.16, 50.44, 55.78, 70.90, 72.28, 178.00 ppm. HRMS (+ESI) calcd for $C_{26}H_{45}O_4$ $(M+H)^+$: 421.3318; found: 421.3316.

4.1.5. 3α,7α-Diformyloxy-6α-ethyl-5β-cholan-24-oic acid (8)

6-ECDCA (**2**) (0.90 g, 2.14 mmol) was dissolved in 30 mL of benzene and treated with *p*-toluenesulfonic acid (0.33 g, 1.73 mmol) and formic acid 99% (5.5 mL). The resulting solution was azeotropically distilled for 2 h using Dean-Stark apparatus. After evaporation of the solvent, the residue was taken up into a mixture of EtOAc/water, extracted with EtOAc (3 × 30 mL), dried, filtered and concentrated on vacuum to obtain 0.82 g (1.71 mmol, 96%) of compound **8** which was used for the next step without further purifications. R_f 0.51 ($CHCl_3$/MeOH, 9:1); ^{1}H NMR (200 MHz, $CDCl_3$) δ 0.65 (s, 3H, 18-*CH*$_3$), 0.79-0.95 (m, 9H, 19-CH_3, 21-CH_3 and 2′-CH_3), 4.61-4.96 (m, 1H, 3-*CH*), 5.18 (m, 1H, 7-*CH*), 8.04 (s, 1H, C*H*O), 8.15 ppm (s, 1H, C*H*O). HRMS (+ESI) calcd for $C_{28}H_{44}NO_5$ $(M+H)^+$: 474.3219; found: 474.3215.

4.1.6. 23-*N*-(Carbocinnamyloxy)-3α,7α-dihydroxy-6α-ethyl-24-nor-5β-cholan-23-amine (4)

3α,7α-Diformyloxy-6α-ethyl-5β-cholan-24-oic acid (**8**) (0.82 g, 1.71 mmol) was treated with oxalyl chloride (8.0 mL) and reacted at 45 °C for 2 h under nitrogen atmosphere. Removal of the excess of oxalyl chloride by evaporation gave the corresponding acyl chloride, which was dissolved in dry acetone (8 mL). A solution of NaN_3 (0.67 g, 10.26 mmol) in water (4 mL) was added to the acyl chloride solution at 0–5 °C, and the resulting reaction mixture was stirred for an additional 3 h at the same temperature. The solvents were removed, and the residue was poured into cold water (25 mL) and extracted with Et_2O (3 × 20 mL). The combined organic phases were dried over anhydrous Na_2SO_4 and evaporated to obtain the corresponding acyl azide (IR, 2134 and 2267 cm^{-1}). The acyl azide intermediate so obtained was then refluxed in dry toluene (20 mL) for 5 h. To the resulting solution isocyanate derivative **9** (IR 2271 cm^{-1}) *t*-cinnamyl alcohol (0.30 g, 2.05 mmol) was added at the same temperature under nitrogen atmosphere. The end of the reactions was checked by TLC. The reaction mixture was then poured into water (20 mL), the organic phase was separated, and the aqueous phase was extracted with EtOAc (3 × 20 mL). The combined organic phases were washed with brine, dried (Na_2SO_4), filtered, and concentrated under vacuum. The crude 23-*N*-(carbocinnamyloxy)-3α,7α-diformyloxy-6α-ethyl-24-nor-5β-cholan-23-amine was then treated overnight with a saturated methanolic solution of K_2CO_3 (20 mL) at room temperature. After evaporation of the solvent, the residues were dissolved in water (20 mL), acidified with 2 N HCl, and extracted with CH_2Cl_2 (3 × 20 mL). The combined organic extracts were dried over anhydrous Na_2SO_4, filtered, concentrated under vacuum. The residual was purified by silica gel flash chromatography using a mixture of CH_2Cl_2/MeOH as eluent, affording the desired compound **4** as a white solid (0.82 g, 1.49 mmol, 87%). R_f 0.18 ($CHCl_3$/MeOH, 96:4); mp: 88-92 °C; ^{1}H NMR (400 MHz, $CDCl_3$) δ 0.64 (s, 3H, 18-*CH*$_3$), 0.91-0.88 (m, 6H, 19-CH_3 e 2′-*C*H$_3$), 0.96 (d, J = 6 Hz, 3H, 21-CH_3), 3.13 (m, 1H, 23-CH), 3.26 (m, 1H, 23-CH), 3.40 (m, 1H, 3-CH), 3.68 (s, 1H, 7-CH), 4.71 (d, J = 5.6 Hz, 2H, *CH*$_2$–CH=CH–C_6H_5), 6.29-6.31 (m, 1H, CH_2–*CH*=CH–C_6H_5), 6.62-6.66 (d, J = 16 Hz, 1H, CH_2–CH=*CH*–C_6H_5), 7.25-7.39 ppm (m, 5H, *Ph*); ^{13}C NMR (100.6 MHz, $CDCl_3$) δ 11.65, 11.72, 18.59, 20.69, 22.19, 23.11, 23.64, 28.34, 30.58, 33.17, 33.76, 33.92, 35.46(×2), 36.04, 38.63, 39.55, 39.96, 41.13, 42.72, 45.14, 50.46, 55.96, 65.27, 70.83, 72.28, 124.01, 126.56, 127.90, 128.54, 133.52, 136.32, 156.26 ppm; IR (KBr): ν = 3355.05, 2927.90, 1701.39, 1525.90, 1448.28, 1256.88, 1133.46, 1060.17, 967.61 cm^{-1}. HRMS (+ESI) calcd for $C_{35}H_{53}NO_4$ $(M+H)^+$: 552.4053; found: 552.4051.

4.2. Biology

4.2.1. FXR Alphascreen assay

Activity on FXR was assayed by using Alphascreen technology in a coactivator recruitment assay. Anti-GST-coated Acceptor beads were used to capture the GST-fusion FXR-LBD whereas the biotinylated-SRC-1 peptide was captured by the streptavidin Donor beads. Upon illumination at 680 nm chemical energy is transferred from Donor to Acceptor beads across the complex streptavidin-Donor/Src-1-Biotin/GSTFXR-LBD/Anti-GST-Acceptor and a signal is produced. The assay was performed in white, low-volume, 384-well Optiplates (PerkinElmer) using a final volume of 25 μL containing final concentrations of 10 nM of purified GST-tagged FXR-LBD protein, 30 nM biotinylated Src-1 peptide, 20 μg/ml anti-GST acceptor beads acceptor beads and 10 μg/ml of streptavidin donor bead (PerkinElmer). The assay buffer contained 50 mM Tris (pH 7.4), 50 mM KCl, 0.1% BSA, and 1 mM DTT. The stimulation times with 1 μL of tested compound (solubilized in 100% DMSO) were fixed to 30 min at room temperature. The concentration of

DMSO in each well was maintained at a final concentration of 4%. After the addition of the detection mix (acceptor and donor beads) the plates were incubated in the dark for 4 h at room temperature and then were read in Envision microplate analyzer (PerkinElmer). Dose response curves were done in triplicate and Z′-factor was used to validate the assays. Non linear regression curves, without constraints, were performed by using four parameter equation and GraphPad Prism Software (GraphPad Inc.), to obtain the EC_{50} values.

4.2.2. Cell culture and FXR transactivation assay

HepG2 and HEK293T cells were cultured in E-MEM and DMEM respectively, either supplemented with 1% penicillin/streptomycin, 1% L-glutamine and 10% fetal bovine serum (high glucose) (Invitrogen, Carlsbad, CA). Cells were grown at 37 °C in 5% CO_2. All the transfections were made using 5:2 (volume:weight) of Fugene HD Trasfection reagent (5 μL) to DNA (2 μg), respectively, according to the manufacturer's instructions (Roche). Twenty-four hours before transfection HEK293T or HepG2 cells were seeded onto a 96-well plate at a density of 10,000 or 15,000 cells/well, respectively. Transient transfections were performed using 100 ng of reporter vector pGL4.29[luc2P/CRE/Hygro] (Promega), 40 ng of pGL4.74 (Renilla), as internal control for transfection efficiency, and 10 ng of expression plasmid pCMV-SPORT6-hFXR. The pGEM vector was added to normalize the amounts of DNA transfected in each assay (2 μg). Twenty-four hours post-transfection the cells were stimulated with increasing concentrations of tested compound for 18 h. Control cultures received vehicle (0.1% DMSO) alone. The cells were then lysed by adding 75 μL of Dual-Glo Luciferase Reagent (Promega) to 75 μL of medium containing cells/well. Renilla luciferase activity was measured by adding volume:volume of Dual-Glo Stop & Glo reagent and original culture medium. Luciferase activities were expressed as ratio between luciferase unit and renilla luciferase unit. Each data point is the average of triplicate assays. Each experiment was repeated almost three times.

4.2.3. FXR target gene expression

The mRNA expression level of FXR target genes was measured by Real-Time Polymerase Chain Reaction (Q-RTPCR). Total RNA was isolated (Aurum Total RNA Mini Kit BioRad) from HepG2 cells stimulated with increasing concentration of tested compound for 18 h. The RNA was random reverse-transcribed with Iscript cDNA Synthesis kit (BioRad) in 20 μL reaction volume. Ten ng template was used in 20 μL final volume reaction of Real-Time PCR containing 0.3 μM of each primer and 10 μL of 2X SYBR Green PCR Master MIX (Bio-Rad). All reactions were performed in triplicate and the thermal cycling conditions were: 3 min at 95 °C, followed by 45 cycles of 95 °C for 10 s, and 60 °C for 30 s in iCycler iQ5 instrument (Biorad, Hercules, CA). The mean value of the replicates for each sample was calculated and expressed as cycle threshold (CT: cycle number at which each PCR reaction reaches a predetermined fluorescence threshold, set within the linear range of all reactions). The amount of gene expression was then calculated as the difference (ΔCT) between the CT value of the sample for the target gene and the mean CT value of that sample for the endogenous control. Relative expression was calculated as the difference (ΔΔCT) between the ΔCT values of the test sample and of the control sample (WT) for each target gene. The relative quantization value was expressed and shown as 2-ΔΔCT. All PCR primers were intron spanning designed using the software Beacon Designer on published sequence data from the NCBI database.

4.2.4. TGR5 FRET assay

The receptor activation was assessed by measuring the level of cyclic AMP (cAMP) using FRET assay. Human intestinal cell lines (NCI-H716) were plated in 96-well plates coated with 0.75 mg/ml Matrigel (BD Biosciences) according to manufacturer's instructions just prior to use, at a density of 12×10^3 cells/well in DMEM supplemented with 10% (v/v) FBS, 100 units/ml penicillin and 100 μg/mL streptomycin sulfate, and cultured for 24 h, which allowed cell adhesion to the bottom of the plate. The cells were washed twice with PBS and medium was exchanged for cAMP assay medium [OPTIMEM containing 0.1% (w/v) BSA and 1 mM 3-isobuty1-1-methylxanthine (IBMX)]. After incubation for 60 min. at 37 °C, the cells were treated with increasing concentrations of tested compound in stimulation Buffer (5 mM HEPES, 0.1% BSA in HBSS pH 7.4) containing the europium chelate—Streptavidin and the ALEXA Fluor 647-conjugated antibody anti-cAMP (PerkinElmer) for 1 h at room temperature. The level of intracellular cAMP was determined with Lance kit (PerkinElmer). Lithocholic acid was used as control ligand. Z′-factor was used to validate assays. Non linear regression curves, without constraints, were performed by using four parameter equation and GraphPad Prism Software (GraphPad Inc.), to obtain the EC_{50} values.

4.3. Molecular modeling

All the calculations were performed with the Schrodinger Suite 2008 (Schrodinger Inc., NY, USA). The docked compounds were prepared with the default options of the *LigPrep* module to assign all the possible protonation states at pH 7.0 ± 2. The crystal structure of FXR in complex with 6-ECDCA (pdb code = 1OSV) was used for docking experiments after being prepared with the standard options of the Protein Preparation Wizard protocol. The docking grid was calculated placing the coordinates of the center of mass of the co-crystallized ligand as center of a cubic box, having a side length of 10 Å. All docking calculations were performed using the extra precision (XP) mode of Glide 5.0. The best poses were stored and used for molecular dynamic simulations (MD) that were carried out with Desmond package. In particular, the four resulting complexes were firstly solvated with water TIP3P and neutralized with the proper counterions using the system builder module. The box used was orthorhombic, having each side at a minimum distance of 10 Å from any atom of the complex. The force field used was the OPLS 2005 in an NPT (isothermic-isobaric) environment. The thermostat used was Berendsen type. The dynamic protocol was set in subsequent steps, with the first being a relaxing minimization, then a progressive increase of temperature to reach 300 K in 140 ps, and finally a production run of 10 ns. Frames of the simulation were recorded every 5 ps. The MD trajectories were analyzed using either the simulation event analysis tool, as implemented in Desmond package, and the VMD tools.

Acknowledgments

This work was supported by Intercept Pharmaceuticals (New York, NY). Thanks are due also to Erregierre (Bergamo, Italy) for the gift of bile acids as starting materials.

Supplementary data

Supplementary data associated with this article can be found, in the online version, at doi:10.1016/j.bmc.2011.03.004.

References and notes

1. For review see: (a) Crawley, M. L. *Exp. Opin. Ther. Pat.* **2010**, *20*, 1047; (b) Fiorucci, S.; Mencarelli, A.; Distrutti, E.; Palladino, G.; Cipriani, S. *Curr. Med. Chem.* **2010**, *17*, 139; (c) Thomas, C.; Pellicciari, R.; Pruzanski, M.; Auwerx, J.; Schoonjans, K. *Nat. Rev. Drug Disc.* **2009**, *7*, 1; (d) Lefebvre, P.; Cariou, B.; Lien, F.; Kuipers, F.; Staels, B. *Physiol. Rev.* **2009**, *89*, 147; (e) Lee, F. Y.; Lee, H.; Hubbert, M. L.; Edwards, P. A.; Zhang, Y. *Trends Biochem. Sci.* **2006**, *31*, 572; (f) Pellicciari, R.; Gioiello, A.; Costantino, G. *Exp. Opin. Ther. Pat.* **2006**, *16*, 333; (g) Pellicciari, R.; Costantino, G.; Fiorucci, S. *J. Med. Chem.* **2005**, *48*, 5383.

2. Forman, B. M.; Goode, E.; Chen, J.; Oro, A. E.; Bradley, D. J.; Perlmann, T.; Noonan, D. J.; Burka, L. T.; McMorris, T.; Lamph, W. W.; Evans, R. M.; Weinberger, C. *Cell* **1995**, *81*, 687.
3. (a) Makishima, M.; Okamoto, A. Y.; Repa, J. J.; Tu, H.; Learned, R. M.; Luk, A.; Hull, M. V.; Lustig, K. D.; Mangelsdorf, D. J.; Shan, B. *Science* **1999**, *284*, 1362; (b) Parks, D. J.; Blanchard, S. G.; Bledsoe, R. K.; Chandra, G.; Consler, T. G.; Kliever, S. A.; Stimmel, J. B.; Willson, T. M.; Zavacki, A. M.; Moore, D. D.; Lehmann, J. M. *Science* **1999**, *284*, 1365; (c) Wang, H.; Chen, J.; Hollister, K.; Sowers, L. C.; Forman, B. M. *Mol. Cell* **1999**, *3*, 543.
4. Inaki, T.; Moschetta, A.; Lee, Y.-K.; Peng, L.; Zhao, G.; Downes, M.; Yu, R. T.; Shelton, J. M.; Richardson, J. A.; Repa, J. J.; Mangelsdorf, D. J.; Kliewer, S. A. *Proc. Natl. Acad. Sci.* **2006**, *103*, 3920.
5. Otte, K.; Kranz, H.; Kober, I.; Thompson, P.; Hoefer, M.; Haubold, B.; Remmel, B.; Voss, H.; Kaiser, C.; Albers, M.; Cheruvallath, Z.; Jackson, D.; Casari, G.; Koegl, M.; Pääbo, S.; Mous, J.; Kremoser, C.; Deuschle, U. *Mol. Cell Biol.* **2003**, *23*, 864.
6. (a) Huber, R. M.; Murphy, K.; Miao, B.; Link, J. R.; Cunningham, M. R.; Rupar, M. J.; Gunyuzlu, P. L.; Haws, T. F.; Kassam, A.; Powell, F.; Hollis, G. F.; Young, P. R.; Mukherjee, R.; Burn, T. C. *Gene* **2002**, *290*, 35; (b) Zhang, Y.; Kast-Woelbern, H. R.; Edwards, P. A. *J. Biol. Chem.* **2003**, *278*, 110.
7. Lee, F. Y.; Lee, H.; Hubbert, M. L.; Edwards, P. A.; Zhang, Y. *Trends Biochem. Sci.* **2006**, *31*, 572.
8. Chen, W. D.; Wang, Y. D.; Zhang, L.; Shiah, S.; Wang, M.; Yang, F.; Yu, D.; Forman, B. M.; Huang, W. *Hepatology* **2010**, *51*, 1.
9. (a) Goodwin, B.; Jones, S. A.; Price, R. R.; Watson, M. A.; McKee, D. D.; Moore, L. B.; Galardi, C.; Wilson, J. G.; Lewis, M. C.; Roth, M. E.; Maloney, P. R.; Willson, T. M.; Kliewer, S. A. *Mol. Cell* **2000**, *6*, 517; (b) Lu, T. T.; Makishima, M.; Repa, J. J.; Schoonjans, K.; Kerr, T. A.; Auwerx, J.; Mangelsdorf, D. J. *Mol. Cell* **2000**, *6*, 507.
10. (a) Jung, D.; Inagaki, T.; Gerard, R. D.; Dawson, P. A.; Kliewer, S. A.; Mangelsdorf, D. J.; Moschetta, A. *J. Lipid Res.* **2007**, *48*, 2693; (b) Inagaki, T.; Choi, M.; Moschetta, A.; Peng, L.; Cummins, C. L.; McDonald, J. G.; Luo, G.; Jones, S. A.; Goodwin, B.; Richardson, J. A.; Gerard, R. D.; Repa, J. J.; Mangelsdorf, D. J.; Kliewer, S. A. *Cell Metab.* **2005**, *2*, 217.
11. Hubbert, M. L.; Zhang, Y.; Lee, F. Y.; Edwards, P. A. *Mol. Endocrinol.* **2007**, *21*, 1359.
12. (a) Ananthanarayanan, M.; Balasubramanian, N.; Makishima, M.; Mangelsdorf, D. J.; Suchy, F. J. *J. Biol. Chem.* **2001**, *276*, 28857; (b) Kast, H. R.; Goodwin, B.; Tarr, P. T.; Jones, S. A.; Anisfeld, A. M.; Stoltz, C. M.; Tontonoz, P.; Kliewer, S.; Willson, T. M.; Edwards, P. A. *J. Biol. Chem.* **2002**, *277*, 2908.
13. (a) Abel, U.; Schlüter, T.; Schulz, A.; Hambruch, E.; Steeneck, C.; Hornberger, M.; Hoffmann, T.; Perović-Ottstadt, S.; Kinzel, O.; Burnet, M.; Deuschle, U.; Kremoser, C. *Bioorg. Med. Chem. Lett.* **2010**, *20*, 4911; (b) Feng, S.; Yang, M.; Zhang, Z.; Wang, Z.; Hong, D.; Richter, H.; Benson, G. M.; Bleicher, K.; Grether, U.; Martin, R. E.; Plancher, J.-M.; Kuhn, B.; Rudolph, M. G.; Chen, L. *Biorg. Med. Chem. Lett.* **2009**, *19*, 2595; (c) Flatt, B.; Martin, R.; Wang, T. L.; Mahaney, P.; Murphy, B.; Gu, X. H.; Foster, P.; Li, J.; Pircher, P.; Petrowski, M.; Schulman, I.; Westin, S.; Wrobel, J.; Yan, G.; Bischoff, E.; Daige, C.; Mohan, R. *J. Med. Chem.* **2009**, *19*, 5289; (d) Deng, G.; Li, W.; Shen, J.; Jiang, H.; Chen, K.; Liu, H. *Bioorg. Med. Chem, Lett.* **2008**, *18*, 5497; (e) Nicolaou, K. C.; Evans, R. M.; Roecker, A. J.; Hughes, R.; Downes, M.; Pfefferkorn, J. A. *Org. Biol. Chem.* **2003**, *1*, 908; (f) Maloney, P. R.; Parks, D.; Haffner, C. D.; Fivush, A. M.; Chandra, G.; Plunket, K. D.; Creech, K. L.; Moore, L. B.; Wilson, J. G.; Lewis, M. C.; Jones, S. A.; Willson, T. M. *J. Med. Chem.* **2000**, *43*, 2971.
14. (a) Iguchi, Y.; Kihira, K.; Nishimaki-Mogami, T.; Une, M. *Steroids* **2010**, *75*, 95; (b) Pellicciari, R.; Gioiello, A.; Costantino, G.; Sadeghpour, B. M.; Rizzo, G.; Meyer, U.; Parks, D. J.; Entrena-Gaudix, A.; Fiorucci, S. *J. Med. Chem.* **2006**, *49*, 4208; (c) Pellicciari, R.; Costantino, G.; Camaioni, E.; Sadeghpour, B. M.; Entrena, A.; Willson, T. M.; Fiorucci, S.; Clerici, C.; Gioiello, A. *J. Med. Chem.* **2004**, *47*, 4559; (d) Fujino, T.; Mizuho, U.; Imanaka, T.; Inoue, K.; Mogami-Nishimaki, T. *J. Lipid Res.* **2004**, *45*, 132; (e) Pellicciari, R.; Fiorucci, S.; Camaioni, E.; Clerici, C.; Costantino, G.; Maloney, P. R.; Morelli, A.; Parks, D. J.; Willson, T. M. *J. Med. Chem.* **2002**, *45*, 3569.
15. Wu, X.; Glickman, J. F.; Bowen, B. R.; Sills, M. A. *J. Biomol. Screen.* **2003**, *8*, 381.
16. (a) Maruyama, T.; Miyamoto, Y.; Nakamura, T.; Tamai, Y.; Okada, H.; Sugiyama, E.; Nakamura, T.; Itadani, H.; Tanaka, K. *Biochem. Biophys. Res. Commun.* **2002**, *298*, 714; (b) Kawamata, Y.; Fujii, R.; Hosoya, M.; Harada, M.; Yoshida, H.; Miwa, M.; Fukusumi, S.; Habata, Y.; Itoh, T.; Shintani, Y.; Hinuma, S.; Fujisawa, Y.; Fujino, M. *J. Biol. Chem.* **2003**, *278*, 9435; (c) Sato, H.; Macchiarulo, A.; Thomas, C.; Gioiello, A.; Une, M.; Hofmann, A. F.; Saladin, R.; Schoonjans, K.; Pellicciari, R.; Auwerx, J. *J. Med. Chem.* **2008**, *51*, 1831; (d) Pellicciari, R.; Sato, H.; Gioiello, A.; Costantino, G.; Macchiarulo, A.; Sadeghpour, B. M.; Giorgi, G.; Schoonjans, K.; Auwerx, J. *J. Med. Chem.* **2007**, *50*, 4265; (e) Pellicciari, R.; Gioiello, A.; Macchiarulo, A.; Thomas, C.; Rosatelli, E.; Natalini, B.; Sardella, R.; Pruzanski, M.; Roda, A.; Pastorini, E.; Schoonjans, K.; Auwerx, J. *J. Med. Chem.* **2009**, *52*, 7958.
17. (a) Montanari, R.; Saccoccia, F.; Scotti, E.; Crestani, M.; Godio, C.; Gilardi, F.; Loiodice, F.; Fracchiolla, G.; Laghezza, A.; Tortorella, P.; Lavecchia, A.; Novellino, E.; Mazza, F.; Aschi, M. G. *J. Med. Chem.* **2008**, *51*, 7768; (b) Bruning, J. B.; Chalmers, M. J.; Prasad, S.; Busby, S. A.; Kamenecka, T. M.; He, Y.; Nettles, K. W.; Griffin, P. R. *Structure* **2007**, *15*, 1258.